Probing Dark Matter via Non-Relativistic Effective Field Theory: WIMP–Nucleus Scattering for Helium target

A. Abid,[1], M. Demirci,[2]*

[1]*Graduate School of Natural and Applied Science, Karadeniz Technical University, Trabzon TR61080, Türkiye*

[2]*Department of Physics, Karadeniz Technical University, Trabzon, TR61080, Türkiye*

Abstract

Non-Relativistic Effective Field Theory (NREFT) provides a systematic framework for studying Weakly Interacting Massive Particles (WIMPs) beyond the conventional spin-independent and spin-dependent paradigms. In this work, we investigate the phenomenology of WIMP-nucleus scattering using a comprehensive set of 15 interaction operators embedded within nuclear response functions. We focus on helium-4 as a target system, motivated by its light mass (4.0026 u), spin-zero ground state ($J = 0$), kinematic matching for low-mass WIMPs (10–50 GeV), and its relevance to emerging superfluid helium technologies. Using the dmscatter code, we compute recoil-energy spectra and event rates for the full NREFT operator basis ($\mathcal{O}_1$–$\mathcal{O}_{15}$). Our results demonstrate that the null spin of ^{4}He strictly suppresses contributions from spin-dependent operators (e.g., $\mathcal{O}_4, \mathcal{O}_6 \to 0$), offering a clean probe for scalar and momentum-dependent interactions. We observe distinct spectral features for momentum-dependent operators such as $\mathcal{O}_3$, $\mathcal{O}_5$, $\mathcal{O}_8$, $\mathcal{O}_{11}$, and $\mathcal{O}_{15}$, alongside the characteristic velocity suppression of $\mathcal{O}_2$ ($v^{\perp} \sim 10^{-3}c$). These findings highlight the complementarity of helium-4 with heavier targets for disentangling NREFT operators and provide essential inputs for interpreting signals in next-generation direct detection experiments.

Keywords: WIMP, NREFT, Dark Matter
DOI: 10.31526/PHEP.2026.20

1. INTRODUCTION

The compelling evidence for dark matter (DM) originates from a wide array of astrophysical and cosmological observations. These include the anomalously flat rotation curves of disk galaxies, velocity dispersion measurements in galaxy clusters, X-ray emissions from hot intracluster gas, gravitational lensing effects, and the large-scale structure of the universe traced by galaxy surveys. Observations of the cosmic microwave background (CMB) anisotropies and baryon acoustic oscillations (BAO) further support the paradigm that non-luminous, non-baryonic matter accounts for approximately 27% of the total energy density of the cosmos. Despite the overwhelming indirect evidence for its gravitational influence, the fundamental particle nature of dark matter remains one of the foremost challenges in modern physics [1, 2, 3, 4].

Weakly Interacting Massive Particles (WIMPs) emerge as favored DM candidates due to their natural production mechanism in the early universe via thermal freeze-out, yielding relic densities consistent with cosmological measurements [5, 6, 7]. Traditional direct detection experiments target WIMP interactions with atomic nuclei predominantly through spin-independent (SI) and spin-dependent (SD) channels, corresponding to coherent scalar and axial-vector couplings, respectively. These interaction modes have been extensively constrained by leading direct-detection experiments such as XENON, LUX/LZ, PandaX, and SuperCDMS, which provide the most stringent experimental upper limits on WIMP–nucleon cross sections over a wide mass range [8, 9, 10, 11, 12]. However, this binary categorization does not encompass the full spectrum of possible interactions predicted by more general frameworks.

The Non-Relativistic Effective Field Theory (NREFT) approach offers a comprehensive, model-independent framework to characterize the full set of hermitian operators governing WIMP–nucleus scattering, constrained only by Galilean invariance and fundamental symmetries [13, 14, 15]. This detailed operator basis translates into nuclear response functions that account for complex nuclear structure effects and interference phenomena beyond the SI and SD approximations. Such theoretical sophistication is crucial for maximizing the sensitivity of direct-detection experiments and correctly interpreting potential signals [16].

In this work, we focus on the helium-4 as a representative light target within the non-relativistic effective field theory framework. Helium-4 is a spin-zero nucleus, implying that all nuclear responses associated with spin-dependent operators vanish identically. This property provides a theoretically clean environment in which scalar and momentum-dependent interactions can be isolated and studied without contamination from spin responses. While operators such as $\mathcal{O}_4$ and $\mathcal{O}_6 \to 0$ formally appear in the NREFT operator basis, their corresponding nuclear responses vanish for helium-4, and the resulting event rates are therefore suppressed to negligible levels. These operators are nevertheless displayed for completeness and to explicitly illustrate the consequences of nuclear spin selection rules. The velocity-suppressed operator $\mathcal{O}_2$ is included to demonstrate the impact of velocity dependence on recoil spectra and to enable a consistent comparison with other momentum-dependent operators such as $\mathcal{O}_3$ and $\mathcal{O}_5$.

*A. Abid: atiquallahabid89@gmail.com
*M. Demirci: mehmetdemirci@ktu.edu.tr

2. THEORETICAL FRAMEWORK

2.1. Differential Event Rate

Direct detection experiments seek to measure nuclear recoil energies from collisions between WIMPs and target nuclei. The expected differential event rate per unit detector mass and nuclear recoil energy is formally expressed as:

$$\frac{dR}{dE_R} = \frac{N_0 \rho_0}{A_m m_\chi} \int_{v_{\min}}^{v_{\rm esc}} v f(\vec{v} + \vec{v}_{\rm Earth}) \, \frac{d\sigma}{dE_R} \, d^3 v, \tag{1}$$

where N_0 is Avogadro's number, ρ_0 is the local dark matter density, A_m is the molar mass of the target nuclei and m_χ is the WIMP mass. The function $f(\vec{v})$ is the velocity distribution and $\vec{v}_{\rm Earth}$ is the velocity of the Earth in the galactic rest frame, the variable v_{min} denotes the minimum WIMP velocity necessary to impart the recoil energy E_R, and $d\sigma/dE_R$ is the differential cross section [17, 18, 19]. The minimum WIMP velocity is given by

$$v_{\min}(E_R) = \frac{q}{2\mu_T} = \frac{1}{\mu_T} \sqrt{\frac{m_T E_R}{2}}, \tag{2}$$

where $\mu_T = \frac{m_T m_\chi}{m_T + m_\chi}$ is the WIMP–nucleus reduced mass and m_T is the nuclear target mass. The WIMP–nucleon momentum transfer is given by $\vec{q} = \vec{p}\,' - \vec{p} = \vec{k} - \vec{k}\,'$, with $\vec{p}\,'$ ($\vec{p}$) being the outgoing (incoming) χ momentum and $\vec{k}\,'$ ($\vec{k}$) the outgoing (incoming) N momentum.

In this work, the DM halo velocity distribution is taken to be the standard halo model (SHM), which is described by an isotropic Maxwell–Boltzmann distribution truncated at the Galactic escape velocity. The velocity distribution in the Galactic rest frame is given by [20, 21, 22]

$$f(\vec{v}) = \frac{1}{(2\pi\sigma_v^2)^{3/2} \, N_{\rm R,esc}} \exp\!\left(-\frac{|\vec{v}|^2}{2\sigma_v^2}\right) \Theta(v_{\rm esc} - |\vec{v}|), \tag{3}$$

where σ_v is the DM velocity dispersion and $N_{R,\rm esc}$ is the normalization factor accounting for the truncation at $v_{\rm esc}$. The normalization constant is

$$N_{R,\rm esc} = \mathrm{erf}\!\left(\frac{v_{\rm esc}}{\sqrt{2}\sigma_v}\right) - \sqrt{\frac{2}{\pi}} \, \frac{v_{\rm esc}}{\sigma_v} \exp\!\left(-\frac{v_{\rm esc}^2}{2\sigma_v^2}\right). \tag{4}$$

In this analysis, we use the commonly adopted SHM parameters: $v_0 = \sqrt{2}\,\sigma_v = 220$ km/s, $v_{\rm esc} = 544$ km/s [23, 24], and a local DM density of $\rho_0 = 0.3\,\mathrm{GeV}/c^2\,\mathrm{cm}^{-3}$.

2.2. Non-Relativistic Effective Field Theory Framework

Traditional analyses of WIMP–nucleon scattering in direct detection experiments focus primarily on spin-independent (SI) and spin-dependent (SD) interactions. While these channels capture the leading contributions in many simple models, they do not exhaust the full set of interaction structures allowed by symmetry principles, and they neglect possible momentum- and velocity-dependent couplings that can significantly affect nuclear recoil spectra [13, 25].

A more general and systematic description is provided by the NREFT framework for dark matter direct detection. In this approach, the WIMP–nucleon interaction is formulated at the level of a non-relativistic effective Hamiltonian, appropriate for elastic scattering at small momentum transfer and non-relativistic velocities. The most general Hamiltonian consistent with Galilean invariance, Hermiticity, and time-reversal symmetry can be written as [13, 14]:

$$\mathcal{H}_{\rm EFT} = \sum_{x=p,n} \sum_{i=1}^{15} c_i^x \, \mathcal{O}_i^x, \tag{5}$$

with coupling coefficients c_i^x, where isoscalar ($\tau = 0$) and isovector ($\tau = 1$) components distinguish proton and neutron couplings [26]:

$$c_i^{(\tau=0)} = \frac{1}{2}(c_i^{x=p} + c_i^{x=n}), \qquad c_i^{(\tau=1)} = \frac{1}{2}(c_i^{x=p} - c_i^{x=n}). \tag{6}$$

The operators $\mathcal{O}_i$ depend explicitly on the nucleon spin operator $\vec{S}_N$, the WIMP spin operator $\vec{S}_\chi$, the momentum transfer $\vec{q}$, and the transverse component of the relative velocity between WIMP and nucleon, $\vec{v}^{\perp}$. The transverse velocity is defined as $\vec{v}^{\perp} = \vec{v} + \vec{q}/(2\mu_T)$ where $\vec{v}$ is the incoming WIMP–nucleon relative velocity and μ_T is the WIMP–nucleon reduced mass. By construction, the transverse velocity satisfies $\vec{v}^{\perp} \cdot \vec{q} = 0$. The standard NREFT operator basis adopted in this work is given by [13, 26]

$$\mathcal{O}_1 = 1_\chi 1_N \tag{7}$$

$$\mathcal{O}_2 = (v^{\perp})^2 \tag{8}$$

$$\mathcal{O}_3 = i\vec{S}_N \cdot \left(\frac{\vec{q}}{m_N} \times \vec{v}^{\perp}\right) \tag{9}$$

$$\mathcal{O}_4 = \vec{S}_\chi \cdot \vec{S}_N \tag{10}$$

$$\mathcal{O}_5 = i\vec{S}_\chi \cdot \left(\frac{\vec{q}}{m_N} \times \vec{v}^{\perp}\right) \tag{11}$$

$$\mathcal{O}_6 = \left(\vec{S}_\chi \cdot \frac{\vec{q}}{m_N}\right)\left(\vec{S}_N \cdot \frac{\vec{q}}{m_N}\right) \tag{12}$$

$$\mathcal{O}_7 = \vec{S}_N \cdot \vec{v}^{\perp} \tag{13}$$

$$\mathcal{O}_8 = \vec{S}_\chi \cdot \vec{v}^{\perp} \tag{14}$$

$$\mathcal{O}_9 = i\vec{S}_\chi \cdot \left(\vec{S}_N \times \frac{\vec{q}}{m_N}\right) \tag{15}$$

$$\mathcal{O}_{10} = i\vec{S}_N \cdot \frac{\vec{q}}{m_N} \tag{16}$$

$$\mathcal{O}_{11} = i\vec{S}_\chi \cdot \frac{\vec{q}}{m_N} \tag{17}$$

$$\mathcal{O}_{12} = \vec{S}_\chi \cdot \left(\vec{S}_N \times \vec{v}^{\perp}\right) \tag{18}$$

$$\mathcal{O}_{13} = i\left(\vec{S}_\chi \cdot \vec{v}^{\perp}\right)\left(\vec{S}_N \cdot \frac{\vec{q}}{m_N}\right) \tag{19}$$

$$\mathcal{O}_{14} = i\left(\vec{S}_\chi \cdot \frac{\vec{q}}{m_N}\right)\left(\vec{S}_N \cdot \vec{v}^{\perp}\right) \tag{20}$$

$$\mathcal{O}_{15} = -\left(\vec{S}_\chi \cdot \frac{\vec{q}}{m_N}\right)\left(\left(\vec{S}_N \times \vec{v}^{\perp}\right) \cdot \frac{\vec{q}}{m_N}\right) \tag{21}$$

Within this operator basis, the conventional spin-independent and spin-dependent interactions correspond to the operators $\mathcal{O}_1$ and $\mathcal{O}_4$, respectively [26]. The remaining operators describe interaction structures beyond the SI/SD paradigm, introducing explicit momentum and velocity dependence, as well as non-trivial operator interference effects [27]. The NREFT framework therefore provides a unified and comprehensive description of WIMP–nucleus scattering phenomenology.

2.3. Nuclear Response Functions

Embedding the NREFT operators into nuclear systems yields nuclear matrix elements expressed in terms of nuclear response functions $W_i^{\tau\tau'}(q^2)$. The differential WIMP–nucleus cross section can be written in the standard NREFT form as [13, 26]

$$\frac{d\sigma}{dE_R} = \frac{2m_T}{4\pi v^2} \sum_{\tau,\tau',i,j} c_i^\tau \, c_j^{\tau'*} \, W_{ij}^{\tau\tau'}(q^2), \tag{22}$$

where m_T is the target nucleus mass, and the response functions $W_i^{\tau\tau'}(q^2)$ encode the nuclear structure and depend on the squared momentum transfer q^2. The nuclear response functions reflect the internal nuclear structure and include contributions from mass monopole (SI), spin, orbital angular momentum, and velocity-dependent operators. For a spin-zero nucleus such as helium-4, spin-dependent responses vanish, leading to the suppression of operators sensitive to nuclear spin [26, 28].

Helium as a spin-zero nucleus exhibits vanishing spin-dependent nuclear responses, which leads to the suppression of operators sensitive to nuclear spin:

$$W_\Sigma = W_{\Sigma'} = W_\Delta = W_{\Delta\Sigma} \to 0. \tag{23}$$

Here, W_Σ and $W_{\Sigma'}$ denote the transverse and longitudinal spin response functions associated with axial-vector couplings, while W_Δ and $W_{\Delta\Sigma}$ correspond to orbital angular-momentum and spin–orbit interference responses in the NREFT formalism. These nuclear response functions arise from the multipole expansion of the WIMP–nucleus interaction Hamiltonian and encode the nuclear structure dependence of the scattering amplitude. Their explicit definitions and derivations can be found in [28], where the mapping between effective operators and nuclear response operators is provided. For a spin-zero nucleus such as Helium-4, all spin-dependent responses vanish identically due to the absence of net nuclear spin, leading to the suppression expressed in Eq. (23).

Consequently, only scalar and certain momentum- and velocity-dependent operators produce non-negligible nuclear responses for 4He, effectively selecting $\mathcal{O}_1$ and a subset of operators such as $\mathcal{O}_3$, $\mathcal{O}_5$, $\mathcal{O}_8$, and $\mathcal{O}_{11}$ and $\mathcal{O}_{15}$ in our calculations. This simplifies the theoretical treatment while emphasizing the role of light, spin-zero nuclei as clean probes of non-standard interactions within the NREFT framework. All numerical results were obtained using the DMscatter code with standard halo parameters and publicly available nuclear response functions. The WIMP velocity distribution is assumed to follow a truncated Maxwell–Boltzmann form with parameters specified in Section 3. The numerical setup, operator normalization, and coupling conventions follow those of Refs. [13, 26] enabling full reproducibility of the presented results.

3. NUMERICAL SETUP

All WIMP-nucleus scattering calculations in this work were performed using the dmscatter package [31]. This code implements the complete 15-operator NREFT basis and the associated nuclear response functions. The nuclear structure inputs for helium-4 and germanium-72 were obtained from the default dmscatter nuclear database.

3.1. Astrophysical Parameters

We adopt the Standard Halo Model (SHM) for the galactic dark matter distribution. The astrophysical parameters are fixed as follows: a local dark matter density of $\rho_0 = 0.3\ \mathrm{GeV}/c^2\mathrm{cm}^{-3}$, a local circular velocity of $v_0 = 220\ \mathrm{km\ s}^{-1}$, and a Galactic escape velocity of $v_{\mathrm{esc}} = 544\ \mathrm{km\ s}^{-1}$. The velocity distribution is modeled as a Maxwellian distribution truncated at v_{esc}, explicitly accounting for the Earth's velocity relative to the halo.

3.2. Coupling Benchmarks and Analysis Strategy

To provide a comprehensive analysis of the scattering phenomenology, we employed two distinct coupling strategies corresponding to the results presented in Section 4:

- **Isoscalar Benchmark (Figure 1):** For the comparative analysis of target complementarity and WIMP mass dependence, we assumed an isoscalar coupling scenario in which the proton and neutron coefficients are equal ($c_p = c_n$). A benchmark coupling strength of $c_p = c_n = 4.8 \times 10^{-4}$ was adopted. This value is a common reference in the literature to facilitate qualitative comparisons between light and heavy targets without loss of generality.
- **Single Operator Dominance (Figure 2):** To isolate the spectral shape and energy dependence characteristic of each interaction type, we applied the "single operator dominance" ansatz. In this mode, the proton coupling for the specific operator under investigation ($\mathcal{O}_i$) is normalized to unity ($c_p = 1$), while the neutron coupling and all other operator coefficients are set to zero ($c_n = 0$). WIMP masses were fixed at benchmark values of 50 GeV and 100 GeV for this detailed spectral breakdown.

3.3. Output Units and Reproducibility

The fundamental differential event rates are initially computed in units of events/kg/day/keV. To illustrate the experimental sensitivity for a realistic detector setup, the spectra presented in this work are scaled by a benchmark exposure of 2500 kg-days and converted to differential rates per MeV. Consequently, the vertical axes in the figures represent the expected number of events per unit energy, expressed in events/MeV, while the recoil energy is displayed in keV to resolve low-energy features.

The input configurations for dmscatter, including the specific isospin structures and operator coefficients defined above, strictly follow the conventions outlined in Ref. [31]. These numerical definitions, combined with the theoretical formalism in Section 2, constitute a sufficient set of parameters to reproduce the results of this study fully.

4. RESULTS AND DISCUSSION

4.1. Helium Target Motivation and Complementarity

In Figure 1, we present the differential event rates as a function of recoil energy for WIMP scattering off ^{4}He (left panel) and ^{72}Ge (right panel). These results assume the isoscalar benchmark scenario ($c_p = c_n$) defined in Section 3, covering WIMP masses of $m_\chi = 25, 50, 100$, and 500 GeV.

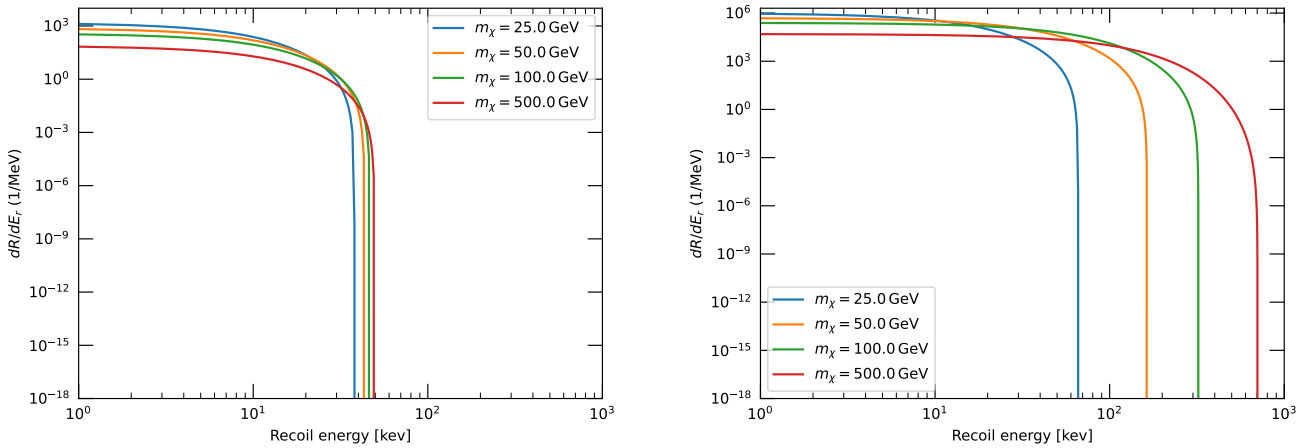

(a) (b)

FIGURE 1: Event rate (per MeV) as a function of recoil energy for several WIMP masses, shown for ^{4}He (a) and ^{72}Ge (b) targets.

At low recoil energies (< 10 keV), the spectra for different WIMP masses cluster closely together for both targets, indicating a weak dependence on WIMP mass in the low-momentum transfer regime. However, as recoil energy increases, distinct kinematic behaviors emerge. For the light helium target ($m_N \approx 3.7$ GeV), the recoil spectra exhibit a smooth, exponential-like decline. This featureless profile reflects the simple nuclear structure of helium-4 and the absence of severe form-factor suppression over the relevant momentum range.

In contrast, the heavier germanium-72 nucleus shows a more pronounced separation between WIMP masses at higher recoil energies. Furthermore, the Ge spectra display visible curvature, attributable to stronger form-factor suppression (Helm form factor) and sharper kinematic cut-offs. This comparison numerically validates the complementarity between target materials: while heavy nuclei such as germanium and xenon offer enhanced sensitivity to high-mass WIMPs and rich form-factor structures, light nuclei such as helium-4 provide a pristine probe for low-energy recoils and light-to-intermediate mass WIMPs, minimizing signal loss due to nuclear structure suppression. This qualitative complementarity is a general feature of elastic WIMP–nucleus scattering and has been extensively discussed in the literature [29, 30]. Helium-4 is therefore well suited to probe low-energy recoils and light to intermediate WIMP masses, while heavier nuclei are more sensitive to higher-mass WIMPs and exhibit richer structure from nuclear form factors. This complementarity has been emphasized in several NREFT analyses and underscores the value of including helium in a global direct-detection program.

From an experimental perspective, helium-based targets are receiving growing attention in next-generation dark matter direct-detection experiments due to their excellent sensitivity to low-mass WIMPs and ultra-low energy thresholds. In particular, superfluid helium detectors have been proposed as promising technologies capable of detecting sub-keV nuclear recoils via quantum evaporation and phonon–roton excitations. Several experimental efforts and detector concepts explore the use of helium as an active target for dark matter searches, demonstrating its potential as a complementary probe to conventional heavy-nucleus detectors [32, 33, 34]. These developments motivate the study of Helium-4 within the NREFT framework as a realistic and experimentally relevant target nucleus for direct detection.

4.2. *Operator-by-Operator Recoil Spectra*

In Figure 2, we present the event rate for 50 GeV and 100 GeV WIMPs interacting with helium nuclei for all 15 NREFT operators. These spectra use the single-operator dominance ansatz described in Section 3, in which specific proton couplings are set to unity ($c_p = 1$) to isolate the kinematic signature of each interaction.

The results visually demonstrate the rigorous selection rules imposed by the Helium-4 nuclear ground state ($J = 0$). As evident from the flat lines in the corresponding panels, the event rates for operators $\mathcal{O}_4, \mathcal{O}_6, \mathcal{O}_7, \mathcal{O}_9, \mathcal{O}_{10}, \mathcal{O}_{13}$, and $\mathcal{O}_{14}$ vanish (falling to numerical noise levels $\sim 10^{-20}$). This confirms that interactions strictly dependent on the nuclear spin operator $\vec{S}_N$ do not contribute to scattering off the spin-zero ^{4}He target.

For the remaining operators that generate observable recoil spectra ($\mathcal{O}_1, \mathcal{O}_2, \mathcal{O}_3, \mathcal{O}_5, \mathcal{O}_8, \mathcal{O}_{11}, \mathcal{O}_{12}, \mathcal{O}_{15}$), we observe three distinct spectral behaviors:

- **Standard and Coherent Interactions ($\mathcal{O}_1, \mathcal{O}_{11}$):** The standard spin-independent operator $\mathcal{O}_1$ and the charge-coherent operator $\mathcal{O}_{11}$ exhibit maximum rates at low recoil energies, followed by an exponential-like decay driven by the nuclear form factor. These operators benefit from the full coherent enhancement of the nucleus.

- **Momentum-Dependent and Transverse Responses ($\mathcal{O}_3$, $\mathcal{O}_5, \mathcal{O}_8, \mathcal{O}_{12}, \mathcal{O}_{15}$):** These operators display richer spectral features. Unlike the monotonic decline of $\mathcal{O}_1$, operators such as $\mathcal{O}_5$, $\mathcal{O}_8$, and $\mathcal{O}_{15}$ show flatter spectra at low energies or distinct curvature before the kinematic cut-off. This behavior arises from their explicit dependence on the momentum transfer $\vec{q}$ and transverse velocity $\vec{v}^{\perp}$, allowing He-4 to probe dark matter particle properties that are inaccessible to standard SI analysis. Remarkably,

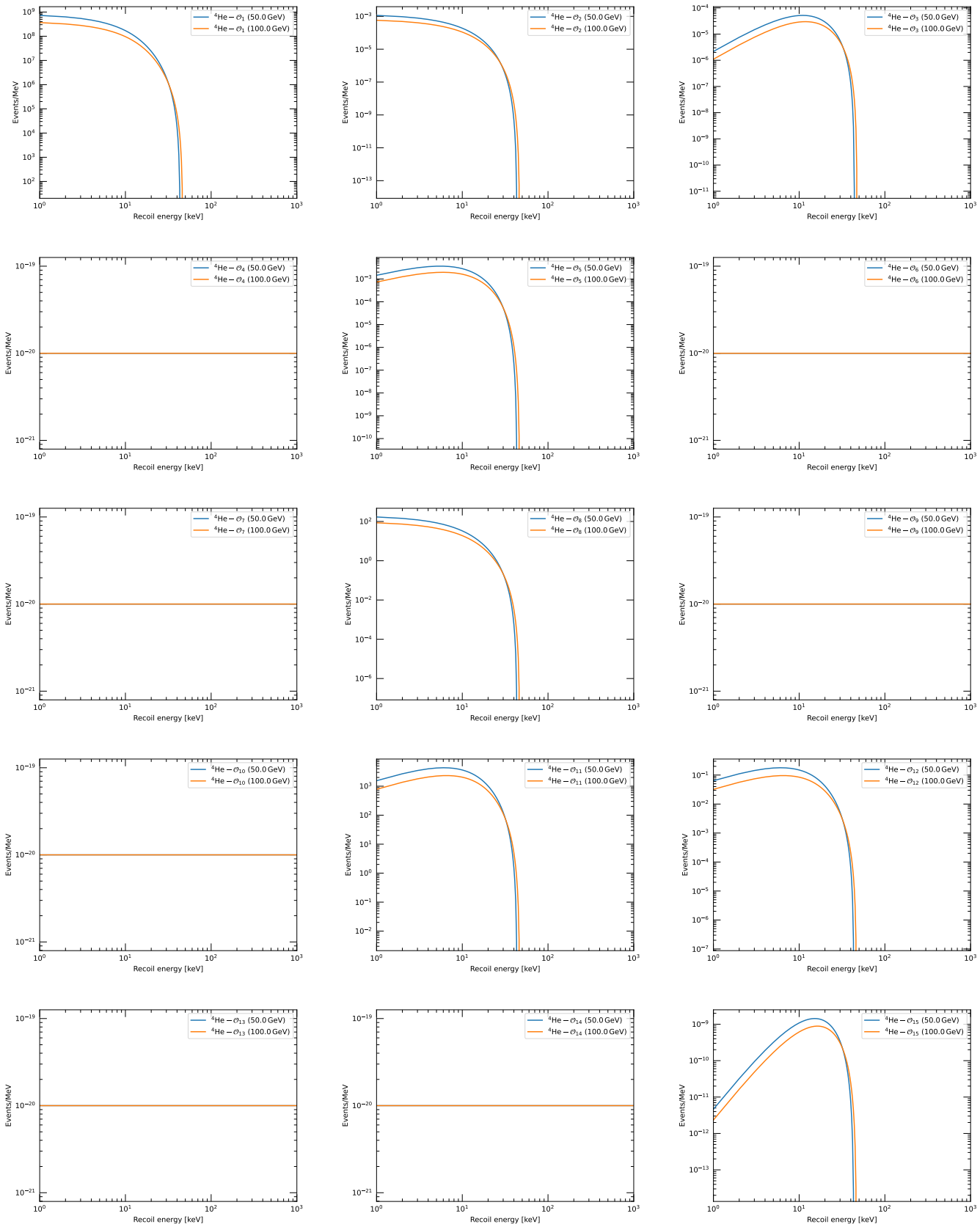

FIGURE 2: Recoil spectra for 15 EFT operators $\mathcal{O}_1$–$\mathcal{O}_{15}$ describing WIMP scattering off ^{4}He nuclei, shown for two representative WIMP masses, 50 GeV and 100 GeV.

while $\mathcal{O}_{12}$ is typically constrained by spin-dependent responses in heavy nuclei, it exhibits a significant non-zero contribution in helium-4 via the spin-orbit interaction, in stark contrast to the vanishing $\mathcal{O}_{13}$.

- **Velocity Suppressed Interaction ($\mathcal{O}_2$):** The spectrum for $\mathcal{O}_2$ mirrors the shape of $\mathcal{O}_1$ but is suppressed by several orders of magnitude in overall rate. This suppression is a direct consequence of the operator's dependence on $(v^{\perp})^2$, which is penalized by the small galactic WIMP velocities ($v/c \sim 10^{-3}$).

Comparing the 50 GeV and 100 GeV mass cases across all non-vanishing operators, the spectral shapes remain qualitatively conserved, with the primary difference being the extension of the recoil tail to higher energies for the heavier WIMP mass.

4.3. Interference Effects and Theoretical Implications

While the results in Figure 2 focus on single-operator dominance to catalog the basis functions, the NREFT formalism naturally allows for interference between operators. In the context of helium-4, the vanishing of spin-dependent responses (W_{SD}) eliminates interference terms involving spin operators (e.g., $\mathcal{O}_4$-$\mathcal{O}_6$ interference).

However, significant interference can still arise in the coherent sector. Specifically, interference between the standard scalar operator $\mathcal{O}_1$ and momentum-dependent operators such as $\mathcal{O}_{11}$ (associated with charge-coherent scattering) or $\mathcal{O}_8$ can constructively or destructively modify the total differential cross-section. Although we have isolated the operators here for clarity, a complete analysis of experimental data would require fitting the full interference terms contained within the $W_M(q^2)$ and Φ'' response functions implemented in the dmscatter framework.

5. CONCLUSION

The NREFT framework represents a powerful, model-independent paradigm for studying WIMP–nucleus interactions, extending beyond conventional SI and SD descriptions by incorporating the full set of Galilean-invariant Hermitian operators and their corresponding nuclear response functions. For a light, spin-zero target such as helium-4, the vanishing of spin-dependent responses simplifies the nuclear structure landscape and isolates the role of scalar and momentum- or velocity-dependent operators. Our results demonstrate that helium-4 provides clean recoil spectra and is particularly informative for probing non-standard interactions associated with operators such as $\mathcal{O}_5$, $\mathcal{O}_8$, $\mathcal{O}_{11}$, $\mathcal{O}_{12}$ and $\mathcal{O}_{15}$, although operators like $\mathcal{O}_2$ remain strongly suppressed due to the small halo velocities. By employing the DMscatter code within the NREFT framework, we compute recoil energy spectra for WIMPs of masses 50 GeV and 100 GeV scattering off helium-4 nuclei, with well-specified astrophysical parameters, couplings, and units, and with an explicit operator basis consistent with the foundational literature. This comprehensive characterization reinforces helium's potential as a viable and informative target nucleus in the search for dark matter, particularly in complementarity with heavier targets. Future work could extend these studies to incorporate additional nuclear targets, include more detailed interference scans in coupling space, and consider subleading nuclear effects to further to refine direct detection strategies within the NREFT approach.

References

[1] L. E. Strigari, *Galactic searches for dark matter*, Phys. Rep. 531 (2013) 188.

[2] K. G. Begeman, A. H. Broeils, R. H. Sanders, *Extended rotation curves of spiral galaxies*, MNRAS 249 (1991) 523.

[3] R. H. Sanders, *The Dark Matter Problem: A Historical Perspective*, Cambridge Univ. Press (2010).

[4] F. Zwicky, *On the Masses of Nebulae and of Clusters of Nebulae*, ApJ 86 (1937) 217.

[5] E. W. Kolb, M. S. Turner, *The Early Universe*, Vol. 69 (1990).

[6] G. Bertone, D. Hooper, *History of dark matter*, Rev. Mod. Phys. 90 (2018).

[7] R. Bandiera, R. Maiolino, *Proceedings, 21st Texas Symposium on Relativistic Astrophysics* (2002).

[8] M. Schumann, *Direct detection of WIMP dark matter: concepts and status*, Journal of Physics G: Nuclear and Particle Physics, 46(10), 103003 (2019).

[9] E. Aprile et. al., (XENON Collaboration), *Dark matter search results from a one ton-year exposure of XENON1T*, Phys. Rev. Lett., 121(11), 111302 (2018).

[10] Aalbers, J., et. al. (LUX-ZEPLIN Collaboration), *First dark matter search results from the LUX-ZEPLIN (LZ) experiment*, Phys. Rev. Lett., 131(4), 041002 (2023).

[11] S. Li, et. al. (PandaX Collaboration). *Search for light dark matter with ionization signals in the PandaX-4T experiment*, Phys. Rev. Lett., 130(26), 261001 (2023).

[12] S. Cebrián, *Review on dark matter searches*, Journal of Physics: Conference Series (Vol. 2502, No. 1, p. 012004). IOP Publishing, (2023).

[13] A. L. Fitzpatrick, W. Haxton, E. Katz, N. Lubbers, and Y. Xu,. *The effective field theory of dark matter direct detection*, JCAP 02, 004 (2013).

[14] N. Anand, A. L. Fitzpatrick, W. C. Haxton, *Weakly interacting massive particle-nucleus elastic scattering response*, Phys. Rev. C,89, 065501 (2014).

[15] S. Kang, S. Scopel, G. Tomar, and J. H. Yoon, *Present and projected sensitivities of Dark Matter direct detection experiments to effective WIMP-nucleus couplings*, Astropart. Phys. 109, 50-68 (2019).

[16] A. Brenner, G. Herrera, A. Ibarra, S. Kang, S. Scopel, and G. Tomar, *Complementarity of experiments in probing the nonrelativistic effective theory of dark matter-nucleon interactions*, JCAP 06, 026 (2022).

[17] M. Schumann, *Direct detection of WIMP dark matter: concepts and status*, J.Phys.G 46 (2019) 10, 103003.

[18] P. Cushman, C. Galbiati, D. N. McKinsey, H. Robertson, and T. M. P. Tait, *Working group report: WIMP dark matter direct detection*, arXiv: 1310.8327 [hep-ex] (FERMILAB-CONF-13-688-AE). Fermi National Accelerator Lab.(FNAL), Batavia, IL (United States) (2013).

[19] A. H. Peter, V. Gluscevic, A. M. Green, B. J. Kavanagh, and S. K. Lee, *WIMP physics with ensembles of direct-detection experiments*, Phys.Dark Univ. 5-6 (2014) 45-74.

[20] A. K. Drukier, K. Freese, and D. N. Spergel. *Detecting cold dark-matter candidates*, Phys. Rev. D 33, 3495-3508 (1986).

[21] N.W. Evans, C.A.J. O'Hare, C. McCabe, *Refinementof the standard halo model for dark matter searches in light of the Gaia Sausage*, Phys. Rev.D 99, 023012 (2019).

[22] C.A.J. O'Hare, N.W. Evans, C. McCabe, G. Myeong,V. Belokurov, *Velocity substructure from Gaia anddirect searches for dark matter*, Phys. Rev. D101, 023006 (2020).

[23] M. C. Smith et al., *The RAVE Survey: Constraining the Local Galactic Escape Speed*, Mon. Not. Roy. Astron. Soc. 379 (2007), 755–772.

[24] L. Necib and T. Lin, *Substructure at High Speed. I. Inferring the Escape Velocity inthe Presence of Kinematic Substructure*. Astrophys. J. 926.2 (2022), 188.

[25] J. Fan, M. Reece, and L. T. Wang, *Non-relativistic effective theory of dark matter direct detection*, JCAP 11 (2010) 042 .

[26] N. Anand, A. L. Fitzpatrick, and W. C. Haxton, *Weakly interacting massive particle-nucleus elastic scattering response*, Phys. Rev. C 89, 065501 (2014).

[27] K. Schneck, et. al. (SuperCDMS Collaboration), *Dark matter effective field theory scattering in direct detection experiments*, Phys. Rev. D 91, 092004 (2015).

[28] R. Catena and B. Schwabe, *Form factors for dark matter capture by the Sun in effective theories*, JCAP 04 (2015) 042.

[29] J. D. Lewin, and P. F. Smith, *Review of mathematics, numerical factors, and corrections for dark matter experiments based on elastic nuclear recoil*, Astropart.Phys. 6, 87-112 (1996).

[30] D. G. Cerdeño, C. Cuesta, M. Fornasa, E. García, C. Ginestra, J. H. Huh, et. al., *Complementarity of dark matter direct detection: the role of bolometric targets*, JCAP 07 (2013) 028, JCAP 09 (2013) E01 (erratum).

[31] O. C. Gorton et al., *dmscatter: A fast program for WIMP-nucleus scattering*, Comput. Phys. Commun. 284 (2023) 108597.

[32] K. Schutz, K. M. Zurek, *Detectability of light dark matter with superfluid helium*, Phys. Rev. Lett. 117(12), 121302 (2016).

[33] K. Matchev, J. Smolinsky, W. Xue, Y. You, *Superfluid effective field theory for dark matter direct detection*, Journal of High Energy Physics, 2022(5), 34 (2022).

[34] S. A. Hertel, A. Biekert, J. Lin, V. Velan, D. N. McKinsey, *Direct detection of sub-GeV dark matter using a superfluid He 4 target*, Phys. Rev. D, 100(9), 092007 (2019).

[35] R. Catena, *Phenomenology of dark matter-nucleon effective interactions*, J. Phys. Conf. Ser. 718 (2016) 4, 042012.